Short Papers

On the Evaluation of the Double Surface Integrals Arising in the Application of the Boundary Integral Method to 3-D Problems

Paolo Arcioni, Marco Bressan, and Luca Perregrini

***Abstract*— In this paper, the authors discuss how to minimize the computing time for the evaluation of the double surface integrals arising in the application of the boundary integral method (BIM) to three-dimensional (3-D) problems. The integrals considered refer to the Green's functions for the scalar and vector potentials and to uniform or linear basis and test functions defined over triangular sub-domains. The authors report original analytical formulas for the double surface integrals over coincident triangles involving the singular terms of the Green's functions and present a criterion for obtaining a good compromise between accuracy and computing time in numerical integration.**

***Index Terms*—Boundary integral method, potential integrals, numerical integration.**

I. Introduction

In the application of the boundary integral method (BIM) to the determination of three-dimensional (3-D) fields in the presence of perfectly conducting bodies, the electromagnetic problem is usually formulated in terms of an electric field integral equation, where the electric field is related to the unknown surface current by the Green's functions for the scalar and vector potentials. Triangular patches in conjunction with the vector basis functions proposed in [1] are commonly used to represent the surface of the bodies and the current distributed thereat. Since many patches are needed when complicated or large structures are to be analyzed, the order of the system matrices deriving from the discretization of the integral equation may be rather large. Moreover, these matrices are dense and their calculation requires the field evaluation in the source region where the kernel of the integral equation diverges. Hence, the time required for the matrice's computation is a substantial part of the total computing time, and its minimization is essential to improve the numerical efficiency.

Many authors applied the BIM to scattering problems, usually with the aim of finding some global parameter, such as the radar cross-section of 3-D objects [1]–[4]. Actually, in these cases quite accurate results can be obtained even with a coarse representation of the field on the surface and/or with a rough estimate of the double surface integrals required for the calculation of the matrices [5]. For this reason, a well-established method to minimize the computing time consists in a first accurate integration, followed by a second, more coarse one, performed by sampling the integrand at a single point.

Recently, the authors used the BIM to calculate the resonant frequencies and the modal fields of cavity resonators [6]. The authors found that in this case the above-mentioned method to evaluate the integrals may lead to quite inaccurate results. In fact, if a good precision (e.g., 0.1%) is required for the resonant frequencies, the matrices calculation must be performed quite carefully (e.g., with an accuracy better than 1%). This paper describes the integration strategy the authors followed to obtain an accurate and fast evaluation of the BIM integrals. The authors report some original analytical formulas for the double surface integrals over coincident triangles involving the singular terms of the Green's functions and discuss the numerical integration scheme. Throughout the paper, reference is made to two different Green's functions, i.e., the quasi-static Green's function for a spherical resonator defined in the Coulomb gauge [7] used in [6], and the free-space Green's function in the Lorentz gauge, widely used in the BIM applications.

Manuscript received June 11, 1995; revised November 21, 1996. This work was supported in part by the Italian National Research Council (CNR) under Contract 92.02857.CT07.

The authors are with the Department of Electronics, University of Pavia, Pavia I-27100 Italy.

Publisher Item Identifier S 0018-9480(97)01722-5.

II. Evaluation of the Integrals

Using the Galerkin's method and the basis functions defined in [1], the integrals required for the evaluation of the matrices have the form

$$\int_T \int_{T'} g(\vec{r},\, \vec{r}\,',\, k)\, dS'\, dS \tag{1}$$

$$\int_T \int_{T'} \vec{\rho}_\alpha \cdot \overleftrightarrow{G}(\vec{r}, \vec{r}\,',\, k) \cdot \vec{\rho}\,'_\beta\, dS'\, dS \tag{2}$$

where T and T' are generic triangular patches, g and $\overleftrightarrow{G}$ are the Green's functions for the scalar and the vector potentials, k is the wavenumber, $\vec{r}$ and $\vec{r}\,'$ denote the field and source points on T and T'; $\vec{\rho}_\alpha = \vec{\rho}_\alpha(\vec{r})$ and $\vec{\rho}\,'_\beta = \vec{\rho}\,'_\beta(\vec{r}\,')$ denote the position vectors of the field and source points with respect to the vertices α and β of the triangles T and T' (see Fig. 1). It is well-known that the Green's functions for the potentials exhibit integrable singularities when the distance $R = |\vec{R}| = |\vec{r} - \vec{r}\,'|$ between the source and the field point vanishes. For this reason, different approaches must be followed according to the following:

- whether T and T' coincide: the integrands in (1) and (2) diverge throughout the whole triangle, and analytical integration of the singular terms is mandatory;
- whether T and T' are joined by an edge or a vertex: the integrands are unbound, a fully numerical integration may fail if a high accuracy is required, and analytical integration of the singular terms is advisable;
- whether T and T' are disjoint triangles: the integrands are bound and smooth, and a Gaussian numerical integration is adequate, the only requirement being a good compromise between accuracy and computation time.

A. Analytical Integration

In the case of coincident or joint triangles the singular parts of the Green's functions in (1) and (2) are extracted and integrated separately. The integrals to be considered are

$$I_1 = \int_T \underbrace{\left[\int_{T'} \frac{1}{R}\, dS'\right]}_{I_4(\vec{r})}\, dS \tag{3}$$

$$I_2 = \int_T \vec{\rho}_\alpha \cdot \underbrace{\left[\int_{T'} \frac{\vec{\rho}\,'_\beta}{R}\, dS'\right]}_{\vec{I}_5(\vec{r})}\, dS \tag{4}$$

$$I_3 = \int_T \vec{\rho}_\alpha \cdot \underbrace{\left[\int_{T'} \frac{1}{R}\left(\overleftrightarrow{I} + \frac{\vec{R}\vec{R}}{R^2}\right) \cdot \vec{\rho}\,'_\beta\, dS'\right]}_{\vec{I}_6(\vec{r})}\, dS \tag{5}$$

TABLE I

ANALYTICAL EXPRESSIONS OF INTEGRALS I_1, I_2, AND I_3 FOR COINCIDENT TRIANGLES: a, b, AND c DENOTE THE LENGTH OF THE EDGES OF THE TRIANGLE; A AND p DENOTE ITS AREA AND HALF-PERIMETER. THE EDGE LABELING IS DIFFERENT FOR THE TWO CASES $\alpha = \beta$ AND $\alpha \neq \beta$

$$I_1 = -\frac{4}{3}A^2\left(\frac{1}{a}\ln(1-\frac{a}{p}) + \frac{1}{b}\ln(1-\frac{b}{p}) + \frac{1}{c}\ln(1-\frac{c}{p})\right)$$

Case $\alpha = \beta$: a is the length of the edge opposite to vertex α

$$I_2 = \frac{A^2}{30}\left[\left(10 + 3\frac{c^2-a^2}{b^2} - 3\frac{a^2-b^2}{c^2}\right)a - \left(5 - 3\frac{a^2-b^2}{c^2} - 2\frac{b^2-c^2}{a^2}\right)b - \left(5 + 3\frac{c^2-a^2}{b^2} + 2\frac{b^2-c^2}{a^2}\right)c + \left(a^2 - 3b^2 - 3c^2 - 8\frac{A^2}{a^2}\right)\frac{2}{a}\ln(1-\frac{a}{p}) + \left(a^2 - 2b^2 - 4c^2 + 6\frac{A^2}{b^2}\right)\frac{4}{b}\ln(1-\frac{b}{p}) + \left(a^2 - 4b^2 - 2c^2 + 6\frac{A^2}{c^2}\right)\frac{4}{c}\ln(1-\frac{c}{p})\right]$$

$$I_3 = \frac{A^2}{15}\left[6\left(4 + \frac{c^2-a^2}{b^2} - \frac{a^2-b^2}{c^2}\right)a - \left(11 - 6\frac{a^2-b^2}{c^2} + \frac{b^2-c^2}{a^2}\right)b - \left(11 + 6\frac{c^2-a^2}{b^2} - \frac{b^2-c^2}{a^2}\right)c + \left(a^2 - 3b^2 - 3c^2 + 4\frac{A^2}{a^2}\right)\frac{2}{a}\ln(1-\frac{a}{p}) + \left(a^2 - 2b^2 - 4c^2 + 12\frac{A^2}{b^2}\right)\frac{4}{b}\ln(1-\frac{b}{p}) + \left(a^2 - 4b^2 - 2c^2 + 12\frac{A^2}{c^2}\right)\frac{4}{c}\ln(1-\frac{c}{p})\right]$$

Case $\alpha \neq \beta$: a is the length of the edge between vertices α and β

$$I_2 = \frac{A^2}{60}\left[\left(-10 + \frac{c^2-a^2}{b^2} - \frac{a^2-b^2}{c^2}\right)a + \left(5 + \frac{a^2-b^2}{c^2} - 6\frac{b^2-c^2}{a^2}\right)b + \left(5 - \frac{c^2-a^2}{b^2} + 6\frac{b^2-c^2}{a^2}\right)c + \left(2a^2 - b^2 - c^2 + 4\frac{A^2}{a^2}\right)\frac{12}{a}\ln(1-\frac{a}{p}) + \left(9a^2 - 3b^2 - c^2 + 4\frac{A^2}{b^2}\right)\frac{2}{b}\ln(1-\frac{b}{p}) + \left(9a^2 - b^2 - 3c^2 + 4\frac{A^2}{c^2}\right)\frac{2}{c}\ln(1-\frac{c}{p})\right]$$

$$I_3 = \frac{A^2}{30}\left[\left(-2 - 3\frac{c^2-a^2}{b^2} + 3\frac{a^2-b^2}{c^2}\right)a + 3\left(1 - \frac{a^2-b^2}{c^2} - 4\frac{b^2-c^2}{a^2}\right)b + 3\left(1 + \frac{c^2-a^2}{b^2} + 4\frac{b^2-c^2}{a^2}\right)c + \left(2a^2 - b^2 - c^2 + 8\frac{A^2}{a^2}\right)\frac{12}{a}\ln(1-\frac{a}{p}) + \left(9a^2 - 3b^2 - c^2 - 12\frac{A^2}{b^2}\right)\frac{2}{b}\ln(1-\frac{b}{p}) + \left(9a^2 - b^2 - 3c^2 - 12\frac{A^2}{c^2}\right)\frac{2}{c}\ln(1-\frac{c}{p})\right]$$

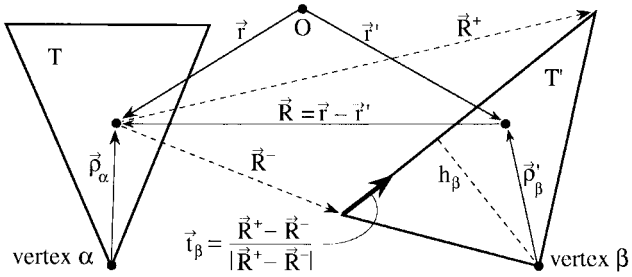

Fig. 1. Geometrical quantities associated to the triangles T and T': h_β is the height of T' with respect to the vertex β.

where $\overleftrightarrow{I}$ is the unit dyadic. Integral I_1 derives from (1), whereas I_2 and I_3 derive from (2), considering the free-space Green's function and the quasi-static spherical resonator Green's function, respectively. The singular terms in (4) and (5) are different due to the different gauge used in defining the vector potential Green's functions [7], [8].

Functions I_4 and $\vec{I}_5$ indicated in (3) and (4) are usually referred to as "potential integrals" and their analytical expressions are reported in [9]–[12]. The authors obtained the analytical expression for $\vec{I}_6$ in (5) substituting the dyadic identity $\vec{R}\vec{R}R^{-3} = \overleftrightarrow{I}\,R^{-1} + \nabla'(\vec{R}R^{-1})$ and applying the Gauss theorem. The authors found

$$\vec{I}_6 = 4\vec{I}_5 - 2(\vec{R} + \vec{\rho}'_\beta)I_4 - \vec{t}_\beta h_\beta(|\vec{R}^+| - |\vec{R}^-|) + (\vec{R}^+ - \vec{t}_\beta\vec{R}^+\cdot\vec{t}_\beta)h_\beta \ln\frac{|\vec{R}^+| + \vec{t}_\beta\cdot\vec{R}^+}{|\vec{R}^-| + \vec{t}_\beta\cdot\vec{R}^-}. \quad (6)$$

The quantities $\vec{R}^+$, $\vec{R}^-$, h_β, $\vec{t}_\beta$ are defined in Fig. 1.

Functions I_4, $\vec{I}_5$, and $\vec{I}_6$ are bound and can be integrated numerically on T to yield I_1, I_2, and I_3. Actually, the authors followed this analytical-numerical integration scheme only for joint triangles since in the case of coincident triangles the authors were able to derive the analytical formulas for I_1, I_2, and I_3 that turned out to be even simpler than the expressions for the potential integrals. Considering two generic coplanar triangles T and T', vectors $\vec{R}$, $\vec{\rho}_\alpha$, and $\vec{\rho}'_\beta$ lie on the same plane of the triangles, and the following identities hold:

$$R^{-1} = -\nabla_s\cdot\nabla'_s R \quad (7)$$

$$\overleftrightarrow{I}R^{-1} = \nabla_s\times\nabla'_s\times\overleftrightarrow{I}R - \nabla_s\nabla'_s R \quad (8)$$

$$\vec{R}\vec{R}R^{-3} = \nabla_s\times\nabla'_s\times\overleftrightarrow{I}R \quad (9)$$

$$\vec{\rho}_\alpha\cdot(\nabla_s\nabla'_s R)\cdot\vec{\rho}'_\beta = \nabla_s\cdot\{\nabla'_s\cdot R[\vec{\rho}_\alpha\vec{\rho}'_\beta + \tfrac{2}{3}(\vec{\rho}_\alpha\vec{R} - \vec{R}\vec{\rho}'_\beta) - \tfrac{4}{9}\overleftrightarrow{I}R^2]\} \quad (10)$$

where ∇_s and ∇'_s are the surface operators—defined over the plane—acting on the unprimed and primed coordinates, respectively. Using these identities and applying the Gauss' and the Stokes' theorems, the double-surface integrals (3)–(5) are transformed into double-line integrals over the boundaries C, C' of T, T'. The authors found:

$$I_1 = -\int_C\int_{C'} R\,\vec{u}\cdot\vec{u}'\,dl\,dl' \quad (11)$$

$$I_2 = -\int_C\int_{C'} R\,\vec{u}\cdot[\vec{\rho}_\alpha\vec{\rho}'_\beta - \vec{\rho}'_\beta\vec{\rho}_\alpha + \tfrac{2}{3}\vec{\rho}_\alpha\vec{R} - \tfrac{2}{3}\vec{R}\vec{\rho}'_\beta + \overleftrightarrow{I}(\vec{\rho}_\alpha\cdot\vec{\rho}'_\beta - \tfrac{4}{9}R^2)]\cdot\vec{u}'\,dl\,dl' \quad (12)$$

$$I_3 = I_2 + \int_C\int_{C'} R\,\vec{u}\cdot(\vec{\rho}'_\beta\vec{\rho}_\alpha - \overleftrightarrow{I}\,\vec{\rho}_\alpha\cdot\vec{\rho}'_\beta)\cdot\vec{u}'\,dl\,dl' \quad (13)$$

where $\vec{u}$ ($\vec{u}'$) is the outward normal to C (C') at $\vec{r}$ ($\vec{r}'$). In the case of coincident triangles the authors could perform the integrals (11)–(13) analytically. After some cumbersome manipulations (not reported here for reasons of space) the authors obtained the expressions reported in Table I (two different formulas are given for I_2 and I_3, according to whether the vertices α and β coincide or not). Note that the expressions in Table I are simple relations involving only the length of the edges, the perimeter, and the area of the triangle.

Incidentally, the authors note that (11)–(13) can be used to evaluate numerically I_1, I_2, and I_3 over coplanar domains of generic shape since in their derivation the triangular shape is immaterial and the integrands are regular functions.

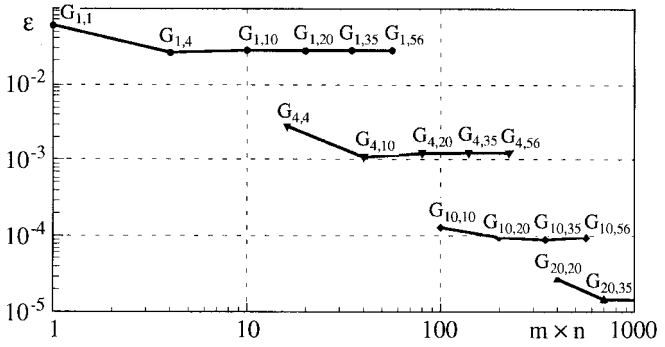

Fig. 2. Maximum relative error ϵ in evaluating (1) by the Gaussian rule $G_{m,n}$ versus the number $m \times n$ of the evaluations of the integrand.

B. Numerical Integration

In performing the numerical integrations the authors used the routine D01PAF of the NAG library [13], which is specialized for triangular domains and implements the n-point ($n = 1, 4, 10, 20, 35, \cdots$) Gaussian quadrature rule, indicated by G_n in the following.

In the case of disjoint triangles, the numerical evaluation of (1), (2) is performed by the Gaussian rule $G_{m,n}$, resulting from the use of G_m on T and G_n on T'. The overall precision depends on m and n, whereas the computing time is proportional to the total number of function evaluations, i.e., to $m \times n$.

To derive the criterion for the best choice of m and n, the authors compared the values of integrals (1) and (2) obtained using different rules $G_{m,n}$ with the values obtained by an accurate adaptive integration. The relative errors were calculated considering a large number of pairs of triangles belonging to fairly regular meshes approximating different surface shapes. In all cases, the mesh size did not exceed a quarter wavelength to adequately represent the current density with the basis functions the authors used [5]. The main results found are:

- the *maximum relative error* pertaining to the rule $G_{m,n}$ in the evaluation of integrals (1) and (2) is practically independent of the frequency, of the Green's function, of the shape of the surface, and of the mesh size;
- the best compromise between accuracy and computing time is achieved when $m = n$ (balanced rules), as evidenced in Fig. 2 for the case of integrals (1).

The first, not obvious, result can be explained considering that the maximum relative error occurs for the integrals involving the closest disjoint triangles since in this case the integrand is maximally uneven. On the other hand, for close triangles the largest contribution derives from the diverging terms of the Green's functions which are independent of either the frequency or the boundary conditions they satisfy. Moreover, the accuracy in evaluating these last contributions depends essentially on the ratio between the dimensions of the triangles and their distance. Therefore, a modification of the mesh size, which causes a local scaling of the geometry, keeps this ratio unchanged and does not affect the maximum relative error. For these reasons, the data reported in Fig. 2 have a general validity and they can be used to choose the rule that assures a given precision with the minimum number of function evaluations. Other results relative to integrals (2) (not reported here for brevity) show a similar behavior with the only difference being errors about twice as large.

The use of the rule $G_{m,n}$ in the integration of the regular part of the Green's functions over coincident or joint triangles gives rise to relative errors that in general are much smaller than those reported in Fig. 2. The authors note, however, that some problems may derive from a possible residual unevenness of the integrand for coincident triangles. For example, the finite part of the scalar free-space Green's function, i.e., $(e^{-jkR} - 1)/4\pi R$, exhibits a tip for $R = 0$. Thus, the rules the authors considered which require the sampling of the function exactly at the tip may not be so accurate. In these cases, a better result could be obtained following the approach proposed in [14], or considering different Gaussian rules, e.g., those reported in [12].

Finally, in the case of joint triangles taken from the same regular meshes, the authors found that the maximum relative error in evaluating I_1 was about 20%, 4%, 1%, 0.5%, and 0.3%, when integrating I_4 by the G_1, G_4, G_{10}, G_{20}, and G_{35} rule, respectively. When calculating I_2 and I_3 by the same rules errors about twice as large were found.

III. Conclusion

The analytical formulas the authors derived and the integration scheme discussed, together with the numerical data reported, can be used to improve the accuracy and reduce the computing time in the evaluation of the double surface integrals arising in the application of the BIM to 3-D problems in conjunction with the basis functions defined in [1]. In the specific application of the BIM to the determination of the resonant frequencies of cavity resonators [6], the authors found that by using the analytical formulas together with the rule $G_{4,4}$ for the double numerical integrals and the rule G_{20} for integrating the potential integrals on joint triangles, the system matrices are evaluated in fairly short computing times to an accuracy better than 1%. This, in turn, permits an overall precision of the order of 0.1% in the resonant frequencies [6] to be obtained.

Acknowledgment

The authors wish to thank Prof. G. Conciauro for the fruitful discussions.

References

[1] S. M. Rao, D. R. Wilton, and A. W. Glisson, "Electromagnetic scattering by surfaces of arbitrary shape," *IEEE Trans. Antennas Propagat.*, vol. AP-30, pp. 409–418, May 1982.

[2] A. W. Glisson and D. R. Wilton, "Simple and efficient numerical methods for problems of electromagnetic radiation and scattering from surfaces," *IEEE Trans. Antennas Propagat.*, vol. AP-28, pp. 593–603, Sept. 1980.

[3] K. Umashankar, A. Taflove, and S. M. Rao, "Electromagnetic scattering by arbitrary shaped three-dimensional homogeneous lossy dielectric bodies," *IEEE Trans. Antennas Propagat.*, vol. AP-34, pp. 758–766, June 1986.

[4] R. F. Harrington, "Boundary integral formulation for homogeneous material bodies," *J. Electromag. Waves Applicat.*, vol. 3, no. 1, pp. 1–15, 1989.

[5] D. H. Schaubert, D. R. Wilton, and A. W. Glisson, "A tetrahedral modeling method for electromagnetic scattering by arbitrarily shaped inhomogeneous dielectric bodies," *IEEE Trans. Antennas Propagat.*, vol. AP-32, pp. 77–85, Jan. 1984.

[6] P. Arcioni, M. Bressan, and L. Perregrini, "A new boundary integral approach to the determination of resonant modes of arbitrarily shaped cavities," *IEEE Trans. Microwave Theory Tech.*, vol. 43, pp. 1848–1856, Aug. 1995.

[7] M. Bressan and G. Conciauro, "Singularity extraction from the electric Green's function for a spherical resonator," *IEEE Trans. Microwave Theory Tech.*, vol. MTT-33, pp. 407–414, May 1985.

[8] J. Van Bladel, *Singular Electromagnetic Fields and Sources.* Oxford, U.K.: Clarendon Press, 1991.

[9] E. E. Okon and R. F. Harrington, "The polarizabilities of electrically small apertures of arbitrary shape," *IEEE Trans. Electromag. Compat.*, vol. EMC-23, pp. 359–366, Nov. 1981.

[10] S. M. Rao, A. W. Glisson, D. R. Wilton, and B. S. Vidula, "A simple numerical solution procedure for static problems involving arbitrary-shaped surfaces," *IEEE Trans. Antennas Propagat.*, vol. AP-27, pp. 604–608, Sept. 1979.

[11] D. R. Wilton, S. M. Rao, A. W. Glisson, D. H. Schaubert, O. M. Al-Bundak, and C. M. Butler, "Potential integrals for uniform and linear source distributions on polygonal and polyhedral domains," *IEEE Trans. Antennas Propagat.*, vol. AP-32, pp. 276–281, Mar. 1984.
[12] R. D. Graglia, "On the numerical integration of the linear shape functions times the 3-D Green's function or its gradient on a plane triangle," *IEEE Trans. Antennas Propagat.*, vol. 41, pp. 1448–1455, Oct. 1993.
[13] Numerical Algorithms Group, in *NAG Library Manual*. Oxford, U.K.: Mayfield House, 1983.
[14] S. Caorsi, D. Moreno, and S. Sidoti, "Theoretical and numerical treatment of surface integrals involving the free-space Green's function," *IEEE Trans. Antennas Propagat.*, vol. 41, pp. 1296–1301, Sept. 1993.

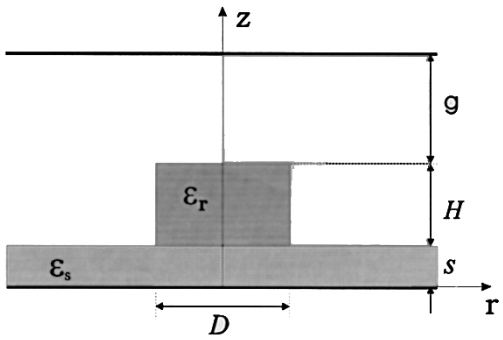

Fig. 1. Configuration of a DR in a MIC environment.

Precise Computations of Resonant Frequencies and Quality Factors for Dielectric Resonators in MIC's with Tuning Elements

Jenn-Ming Guan and Ching-Chuan Su

***Abstract*— In this paper, the highly accurate results of resonant frequencies, field distributions, and quality factors of the $TE_{01\delta}$ mode for the cylindrical shielded dielectric resonator (DR) in monolithic integrated circuits (MIC's) with the practical tuning element, such as the metallic tuning screw and the dielectric tuning device are presented. By using the newly developed FD-SIC method, numerical results can be calculated accurately and efficiently. The DR structures with tuning elements can be more easily modeled by the present approach than the other methods using approximate solutions or the mode-matching (MM) methods. Numerical results in the literature are compared to the present FD-SIC results for the DR without tuning elements and detailed discussions on these results are given. In addition, design curves are also presented for the DR with the metallic tuning screw and with the dielectric tuning device. These design curves are helpful for designing DR systems with tuning elements in MIC applications.**

I. Introduction

Dielectric resonators (DR's) have now become basic components for designing filters and oscillators of high quality factors in many microwave systems. The nature of low-loss and ease of miniaturization into microwave integrated circuits (MIC's) or monolithic microwave integrated circuits (MMIC's) make them very attractive. The state-of-the-art local oscillator design in MIC's often employs DR's to build high-performance DR oscillators. Mechanical tuning elements commonly accompany the DR to change the resonant frequency to compensate for some deviations due to the fabrication tolerance and for some errors due to the theoretical prediction. The typical tuning elements are the metallic tuning plate or screw (Fig. 2) and the dielectric tuning device (Fig. 3). The metallic tuning plate or screw increases the resonant frequency when moved near to the DR, while the dielectric tuning device or another DR is used to decrease the resonant frequency for wide-band usage [1].

Resonant frequencies and field distributions for the DR on the microstrip substrate or in a cavity have been investigated with many numerical methods, such as the effective dielectric constant (EDC) method [2], the mode-matching (MM) methods [3]-[6], the generalized impedance boundary conditions (GIBC's) method [7], the finite-element methods (FEM's) [8], and the frequency-domain finite-difference method [9]. Among them, the simple EDC method [2] is not rigorous and the field distributions obtained are not accurate enough in general, while the rigorous GIBC method [7] is tedious and the results of it are even incorrect in some cases. Numerical results of these two methods will be demonstrated in Section III. Computations of the unloaded quality factor Q_u are usually then performed by the perturbational method via the calculated resonant frequency and field distributions which are obtained from lossless conditions. Literature with this approach includes the EDC method [2] and the one-dimensional (1-D) FEM [10]. On the other hand, quality factors are obtained directly by searching the complex resonant frequencies for the lossy resonators in the MM methods [4]–[6] or by the incremental frequency rule [6]. However, only the basic structure depicted in Fig. 1 is considered in the above-mentioned investigations.

Rigorous calculations for the DR with the metallic tuning screw or the dielectric tuning device are very limited. To the authors' knowledge, only two references can be found: the FEM [8] for only the resonant frequency of the DR with metallic screws and the more complete investigation in [5] by the MM method. The EDC, GIBC, and 1-D FEM methods are not suitable for these two structures. To obtain the precise values of the resonant frequency and Q_u factors of these practical DR systems, efficient and versatile approaches are preferred and needed, especially for the Q_u computation with the perturbational method in which the calculated resonant field distributions should be as correct as possible. In this paper, the finite-difference and simultaneous iteration with the Chebyshev acceleration (FD-SIC) method [9] is extended to model the DR with tuning devices more flexibly. Due to the efficiency of this method, a large number of node points can be used and adequately distributed over the modeling cross sections to calculate the required results precisely.

II. Formulation

The DR placed on the microstrip substrate is shielded by the metallic enclosure, where the side walls are far away from the DR, as indicated in Fig. 1. In actual calculations, the metallic side wall at a large radius is about eight times the radius of the DR. Only the $TE_{01\delta}$ mode is considered for its most common usage in microstrip systems. These DR systems are first assumed to be lossless to obtain the resonant frequencies and eigenfield distributions by using the FD-SIC method [9]. Then, the quality factors are evaluated by the conventional perturbational method in which the surface current densities on the conductor surfaces are related to the magnetic fields

Manuscript received June 11, 1995; revised November 21, 1996.
The authors are with the Department of Electrical Engineering, National Tsinghua University, Hsinchu, Taiwan 30043 R.O.C.
Publisher Item Identifier S 0018-9480(97)01721-3.